

KERNELBAND:Steering LLM-based Kernel Optimization via Hardware-Aware Multi-Armed Bandits

Dezhi Ran^{*12} Shuxiao Xie^{*23} Mingfang Ji²⁴ Anmin Liu¹ Mengzhou Wu¹² Yuan Cao¹² Yuzhe Guo¹²
 Hao Yu⁵ Linyi Li⁶ Yitao Hu⁴ Wei Yang⁷ Tao Xie¹²⁸⁹

Abstract

High-performance GPU kernels are critical for efficient LLM serving, yet their optimization remains a bottleneck requiring deep system expertise. While code LLMs show promise in generating functionally correct code, kernel optimization is intrinsically a search problem over a vast optimization space. The fundamental mismatch prevents existing LLM agents from efficiently exploring the optimization space for diverse hardware and compute patterns. To bridge the gap, we present KERNELBAND, a framework that formulates kernel optimization as a Multi-Armed Bandit (MAB) problem, explicitly balancing exploration and exploitation to unlock the potential of code LLMs. To navigate the infinite arm space of optimization strategies applied to candidate kernels, we design two key mechanisms: a hardware-aware pruning strategy via profiling bounds and a trace-driven clustering algorithm that leverages Lipschitz continuity. Theoretically, we prove that KERNELBAND reduces the regret bound to depend on the compact covering number of runtime clusters, ensuring sample-efficient discovery of high-performance kernels. Extensive experiments on TritonBench-G with three GPU architectures and four code LLMs show that KERNELBAND consistently and substantially outperforms state-of-the-art methods with over 33% average improvement.

^{*}Equal contribution ¹Key Lab of HCST (PKU), MOE; SCS, Peking University, Beijing, China ²Beijing Tongming Lake Information Technology Application Innovation Center, China ³East China Normal University, Shanghai, China ⁴Department of Computer Science, Tianjin University, Tianjin, China ⁵Hong Kong University of Science and Technology, Hong Kong, China ⁶School of Computing Science, Simon Fraser University, Burnaby, BC, Canada ⁷University of Texas at Dallas, USA ⁸Fudan University Institute of Systems for Advanced Computing, China ⁹Shanghai Institute of Systems for Open Computing, China. Correspondence to: Tao Xie <taoxie@pku.edu.cn>.

Preprint. February 12, 2026.

1. Introduction

The computational demands of Large Language Models (LLMs) have grown exponentially (Zhao et al., 2023; Naveed et al., 2025; Floridi & Chiratti, 2020; Team et al., 2025; 2023; Bai et al., 2023), making efficient serving infrastructure a critical priority (Miao et al., 2025; Ye et al., 2025; Kwon et al., 2023; Fang et al., 2021; Yan et al., 2018; Lin et al., 2024; Pan et al., 2024). At the heart of the efficiency lies kernel optimization (Filipović et al., 2015; Ryoo et al., 2008; Lange et al., 2025), the engineering of high-performance primitives for fundamental operations such as attention (Dong et al., 2024) and GEMM (Faingnaert et al., 2021). Traditionally, developing these kernels has been the exclusive domain of specialized experts, requiring careful manual mapping of algorithms to complex hardware features, such as multi-level memory hierarchies and tensor core instructions (NVIDIA, 2025). To democratize this process, domain-specific languages like Triton (Tillet et al., 2019) and TileLang (Wang et al., 2025b) have emerged, offering abstractions that hide low-level intricacies. However, while DSLs simplify implementation, achieving peak performance still relies heavily on compiler autotuning mechanisms to select configuration parameters (Gao et al., 2025; Zhu et al., 2022; Wang et al., 2024). As hardware complexity increases, the configuration space suffers from a combinatorial explosion (Gao et al., 2025; Ansel et al., 2024; Shi et al., 2023), rendering heuristic strategies computationally prohibitive and often incapable of finding global optima within reasonable timeframes.

To circumvent the preceding limitation, the community has recently turned to code LLMs (Dong et al., 2025b; Guo et al., 2024; Hui et al., 2024; Achiam et al., 2023; Caruccio et al., 2024), leveraging their generative capabilities to automate kernel optimization. Current methods primarily fall into two categories: agent-based methods (Dong et al., 2025a; Wang et al., 2025a; Zhang et al., 2025), which use iterative feedback loops to refine implementations, and training-based methods (Baronio et al., 2025; Woo et al., 2025; Kong et al., 2025), which fine-tune models on optimization-specific datasets. However, a fundamental mismatch persists: LLMs are inherently trained to generate statistically probable and

functionally correct code, whereas kernel optimization is intrinsically a search problem over a vast and discontinuous optimization space (Gao et al., 2025). Consequently, existing agents struggle to balance exploration and exploitation, frequently converging to suboptimal local minima or wasting computational resources on invalid configurations, thereby failing to achieve expert-level performance.

To bridge the gap, we present KERNELBAND, the first Multi-Armed Bandit (MAB) (Mahajan & Teneketzis, 2008; Scott, 2010; Boursier & Perchet, 2024; Silva et al., 2022) framework to guide LLMs in navigating the optimization space with provable efficiency, enabled by two novel designs. Distinguished from previous methods (Zhang et al., 2025; Kong et al., 2025) that rely on unguided generation or self-reflection heuristics, KERNELBAND formulates the problem in a contextual bandit setting (Bouneffouf et al., 2020), where each arm corresponds to the application of an optimization strategy (Ryoo et al., 2008) (e.g., tiling, vectorization) to a candidate kernel implementation. To address the challenge of infinite action spaces, we design hardware-aware pruning, which utilizes profiling data to establish tight reward upper bounds, and trace-driven clustering, which exploits the Lipschitz continuity (Hager, 1979) of runtime behaviors to estimate rewards for unexplored arms. Theoretically, we prove that KERNELBAND reduces the regret bound to depend on the compact covering number of runtime clusters rather than the vast kernel space.

We evaluate KERNELBAND on TritonBench-G (Li et al., 2025b) across three GPU architectures (RTX 4090, H20, A100) and four frontier code LLMs (DeepSeek AI, 2025; OpenAI, 2025; Anthropic, 2025; Google, 2025). Empirical results demonstrate consistent superiority over state-of-the-art baselines, achieving up to **1.91**× geometric mean speedup and improving the Fast@1 success rate by **39–140%**. Ablation studies confirm that structured exploration is foundational: replacing our bandit policy with LLM semantic reasoning regresses performance to 0.97× (below the reference kernel), validating that learned execution statistics outperform intuition. Furthermore, KERNELBAND automatically adapts strategies to hardware bottlenecks and delivers **35–50%** higher speedup per dollar than unguided approaches.

This paper makes the following main contributions:

- We propose KERNELBAND, the first framework to formulate LLM-based kernel optimization as a MAB problem, effectively resolving the mismatch between functional code generation and optimization search.
- We design a hardware-aware acquisition strategy that combines profiling-based pruning with trace-driven clustering, proved to efficiently explore the kernel optimization space.

- Extensive experiments on TritonBench-G across three GPUs and four code LLMs demonstrate that KERNELBAND consistently outperforms state-of-the-art methods, achieving up to **1.91**× geometric mean speedup, with ablation results confirming the structured bandit policy as the key to the performance.

2. Problem Formulation

In this section, we formalize kernel optimization as a search problem over a generated code space and subsequently model it as a structured contextual MAB problem with an expanding action space. We explicitly address the mismatch between the generative capabilities of code LLMs (which prioritize functional correctness) and the navigational requirements of kernel optimization (which is intrinsically a search problem over performance landscapes).

2.1. The Search Problem

Given a target hardware platform \mathcal{H} and a naive kernel implementation, we seek a kernel k^* minimizing latency $L(k, \mathcal{H})$ while preserving functional correctness:

$$k^* = \underset{k \in \mathcal{K}_{\text{valid}}}{\operatorname{argmin}} L(k, \mathcal{H}) \quad (1)$$

where $\mathcal{K}_{\text{valid}}$ contains all correct implementations.

We view optimization as traversing a directed graph $\mathcal{G} = (\mathcal{V}, \mathcal{E})$: nodes \mathcal{V} are valid kernels; edges $(k \rightarrow k') \in \mathcal{E}$ represent applying a strategy $s \in \mathcal{S}$ via a code LLM.

The Fundamental Mismatch. While modern Code LLMs excel at generating functionally correct nodes (kernels), they lack the hardware-specific intuition needed to select edges that efficiently navigate toward performance-optimal regions of \mathcal{G} . A naive LLM-based optimizer performs what amounts to a random walk on the graph, wasting substantial efforts on transformations that yield negligible or negative speedups. Our goal is to replace this undirected exploration with a principled decision policy that leverages both program semantics and hardware behavior.

2.2. Contextual Bandit Formulation with Expanding Action Space

We frame kernel optimization as an **iterative frontier expansion** process. Starting from an initial implementation $\mathcal{P}_0 = \{k_{\text{naive}}\}$, at each step t , the agent maintains a frontier $\mathcal{P}_t \subseteq \mathcal{V}$ of promising kernels discovered so far. The core decision is: *which kernel $k \in \mathcal{P}_t$ to expand using which optimization strategy $s \in \mathcal{S}$?*

We formulate this as a **contextual bandit problem** rather than full Reinforcement Learning (RL) for three key reasons: first, optimization trajectories are short, making immediate

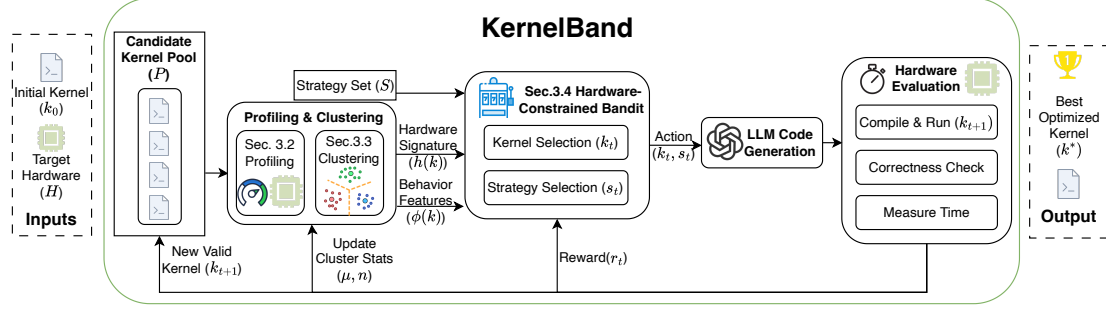


Figure 1. Overview of KERNELBAND. KERNELBAND interleaves runtime analysis (clustering) with hardware-aware decision making (masked bandit) to guide LLM-based kernel optimization.

reward predictive of final performance; second, LLM generation variance complicates long-horizon value estimation; and third, bandits offer rigorous regret bounds under our structural assumptions, ensuring sample efficiency.

Formal Model. We formulate the optimization process as a contextual bandit defined by a tuple of context, action, transition, and reward. The **context space** consists of vectors $x_k \in \mathbb{R}^d$ for each candidate $k \in \mathcal{P}_t$, encoding both static program features and dynamic execution traces $\phi(k)$. The **action space** at time t , denoted $\mathcal{A}_t = \mathcal{P}_t \times \mathcal{S}$, represents applying strategy s to kernel k . Crucially, since the frontier $|\mathcal{P}_t|$ grows with t , \mathcal{A}_t is unbounded, distinguishing this from standard fixed-arm bandits. Executing action $a_t = (k_t, s_t)$ triggers a **generative transition** $k'_t \sim P_{\text{LLM}}(\cdot \mid k_t, s_t, \mathcal{H})$, where stochasticity stems from the LLM’s sampling process. Finally, the agent observes a **reward signal** $r_t \in [0, 1]$ measuring normalized latency improvement: $r_t = \text{Clip}(\frac{L(k_t) - L(k'_t)}{L(k_t)}, 0, 1)$, where zero reward is assigned to performance regressions or compilation failures. The agent’s objective is to maximize the cumulative expected reward $\sum_{t=1}^T \mathbb{E}[r_t]$.

2.3. Structural Properties Enabling Tractable Learning

The expanding action space \mathcal{A}_t poses a fundamental challenge: standard bandit algorithms would suffer linear regret $\mathcal{O}(T)$. However, kernel optimization exhibits two key structural properties that make the problem tractable:

Assumption 1 (Hardware-Aware Gain Boundedness)

The expected improvement from applying strategy s to kernel k is bounded by hardware limits. Formally, there exists a known bounding function (Williams et al., 2009) $B : \mathcal{V} \times \mathcal{S} \rightarrow [0, 1]$ such that:

$$\mu(k, s) \triangleq \mathbb{E}[r_t | k, s] \leq B(k, s) \quad (2)$$

where $B(k, s)$ estimates the maximum achievable gain based on the gap between k ’s current performance and the theoretical limit for strategy s on hardware \mathcal{H} .

Assumption 2 (Lipschitz Continuity in Behavior Space)

The expected reward function $\mu(k, s)$ is Lipschitz continuous with respect to execution behavior. That is, for any strategy s and kernels k_1, k_2 :

$$|\mu(k_1, s) - \mu(k_2, s)| \leq L \cdot \|\phi(k_1) - \phi(k_2)\|_2 \quad (3)$$

where $\phi(k)$ captures runtime characteristics. This implies that kernels with similar bottlenecks respond similarly to optimizations.

Intuition. Together, these assumptions imply that while the code space is infinite, the space of *meaningful optimization decisions* is low-dimensional and structured, motivating the design of KERNELBAND.

3. Methodology: KERNELBAND

3.1. System Overview

As shown in Figure 1, KERNELBAND addresses the challenge of the expanding action space $\mathcal{A}_t = \mathcal{P}_t \times \mathcal{S}$ through three key components: (1) **Runtime behavior characterization** (Sec 3.2), which extracts execution signatures to enable knowledge sharing; (2) **Dynamic clustering** (Sec 3.3), which groups similar kernels to manage the expanding action space; and (3) **Hardware-constrained bandit policy** (Sec 3.4), which selects promising optimizations while pruning physically invalid strategies.

3.2. Runtime Behavior Characterization

We characterize each kernel k using two complementary representations to satisfy the smoothness and boundedness assumptions defined in Section 2.

Behavioral feature vector $\phi(k)$. For clustering kernels with similar optimization responses, we define a 5-dimensional vector $\phi(k)$ comprising normalized execution time $\tilde{T}(k)$ and hardware counters:

$$\phi(k) = [\tilde{T}(k), n_{\text{reg}}, n_{\text{smem}}, d_{\text{block}}, \eta_{\text{occ}}] \quad (4)$$

representing registers per thread, shared memory per block, block dimension, and occupancy, respectively. Kernels close in ϕ -space share similar bottlenecks (Assumption 2), allowing the bandit to generalize strategy performance.

Hardware signature $h(k)$. To implement the bounding function $B(k, s)$ from Assumption 1, we extract a hardware signature $h(k)$ using NVIDIA Nsight Compute (NVIDIA Corporation, 2024), measuring peak throughput percentages for DRAM, L2 cache, and SM. These metrics identify the dominant bottleneck (memory bandwidth/compute/cache) for pruning physically implausible optimization strategies.

3.3. Structured Exploration via Dynamic Clustering

Periodic re-clustering. Instead of maintaining a separate bandit arm for every kernel, we maintain arms for kernel *clusters*. At iteration t , we partition the frontier \mathcal{P}_t into K clusters $\mathcal{C}_t = \{C_1, \dots, C_K\}$ using K-Means on $\{\phi(k)\}$. Clusters are recomputed every τ iterations. This periodic update balances the need to track shifting kernel behaviors with the stability required for bandit convergence.

Representative profiling. Since hardware profiling is expensive (≈ 10 s), we profile only the centroid kernel $k_c^{(i)}$ of each active cluster during the re-clustering phase. We approximate the hardware constraints of the entire cluster using this representative, significantly reducing overhead.

3.4. Hardware-Constrained Bandit Policy

As depicted in Algorithm 1, we formulate the decision process as a *masked bandit*.

Pruning via hardware potential. We define a binary mask $M_{i,s} \in \{0, 1\}$ based on the hardware signature $h(k)$. A strategy s is valid for cluster C_i only if it targets a non-saturated resource:

$$M_{i,s} = \mathbb{I}\left[h(k_c^{(i)})[\text{Target}(s)] < \theta_{\text{sat}}\right] \quad (5)$$

where θ_{sat} is a saturation threshold (e.g., 75%). This reduces the effective action space from $|\mathcal{S}|$ to $|\mathcal{S}_{\text{valid}}|$.

Action selection. At iteration t , we select a cluster-strategy pair (I_t, S_t) using a Masked UCB index. Let $\hat{\mu}_{i,s}$ be the empirical mean reward and $N_{i,s}$ the visit count. We maximize UCB only among valid actions:

$$(I_t, S_t) = \underset{\substack{i \in [K], s \in \mathcal{S} \\ \text{s.t. } M_{i,s}=1}}{\text{argmax}} \left(\hat{\mu}_{i,s} + c \sqrt{\frac{\ln t}{N_{i,s}}} \right) \quad (6)$$

Once (I_t, S_t) is chosen, we sample a specific kernel $k_t \in C_{I_t}$ via a softmax distribution over local potential scores

Algorithm 1 Workflow of KERNELBAND

Require: Kernel k_0 , Strategies \mathcal{S} , Budget T , Period $\tau = 10$, Clusters K

- 1: $\mathcal{P} \leftarrow \{k_0\}$, $\mathcal{C} \leftarrow \{\mathcal{P}\}$ \triangleright Initial single cluster
- 2: Initialize $N_{i,s} \leftarrow 1$, $\hat{\mu}_{i,s} \leftarrow 0.5$ for all i, s
- 3: Initialize Masks $M_{i,s} \leftarrow 1$ \triangleright No pruning initially
- 4: **for** $t = 1$ **to** T **do**
- 5: Compute $\phi(k)$ for all $k \in \mathcal{P}$ \triangleright Periodic clustering & profiling
- 6: **if** $t \bmod \tau = 0$ **and** $|\mathcal{P}| \geq 2K$ **then**
- 7: $\mathcal{C} \leftarrow \text{KMeans}(\{\phi(k)\}, K)$
- 8: Update centroids $k_c^{(i)}$ and profile $h_c^{(i)} \leftarrow \text{NCU}(k_c^{(i)})$
- 9: **end if** \triangleright Hardware-constrained selection
- 10: **if** centroids are profiled **then**
- 11: $M_{i,s} \leftarrow \mathbb{I}[h_c^{(i)}[\text{Target}(s)] < \theta_{\text{sat}}]$
- 12: **end if**
- 13: Select (I_t, S_t) via Eq. (6) (Masked UCB)
- 14: Sample $k_t \in C_{I_t}$ with $P(k) \propto \exp(V_{\text{hw}}(k, S_t))$ \triangleright Generation & update
- 15: $k'_t \leftarrow \text{LLM}(k_t, S_t)$
- 16: **if** Verify(k'_t) **then**
- 17: $r_t \leftarrow \max(0, (\mathcal{T}(k_t) - \mathcal{T}(k'_t)) / \mathcal{T}(k_t))$
- 18: $\mathcal{P} \leftarrow \mathcal{P} \cup \{k'_t\}$
- 19: $N_{I_t, S_t} \leftarrow N_{I_t, S_t} + 1$
- 20: $\hat{\mu}_{I_t, S_t} \leftarrow \hat{\mu}_{I_t, S_t} + \frac{r_t - \hat{\mu}_{I_t, S_t}}{N_{I_t, S_t}}$
- 21: **end if**
- 22: **end if**
- 23: **end for**
- 24: **return** $\arg \min_{k \in \mathcal{P}} \mathcal{T}(k)$

$V_{\text{hw}}(k, S_t) = \theta_{\text{sat}} - h(k)[\text{Target}(S_t)]$, measuring the remaining optimization headroom for strategy S_t on kernel k .

3.5. Theoretical Analysis

We analyze KERNELBAND through the lens of **ϵ -optimality**, acknowledging that in high-dimensional kernel optimization, finding a solution within a small tolerance of the global optimum is the practical goal.

Theorem 1 (Convergence to ϵ -Optimal Solution) *Let μ^* be the optimal performance and r_t be the reward at step t . Under Assumptions 1 and 2, with probability $1 - \delta$, the average regret satisfies:*

$$\frac{1}{T} \sum_{t=1}^T \mathbb{E}[\mu^* - r_t] \leq C \sqrt{\frac{K|\mathcal{S}_{\text{valid}}| \ln T}{T}} + L \cdot \max_i \text{diam}(C_i) \quad (7)$$

where C is a constant derived from the UCB analysis.

Due to space limit, we put the proof in Appendix B.

3.6. Implementation Details

We employ $|\mathcal{S}| = 6$ optimization strategies: *tiling*, *vectorization*, *fusion*, *pipeline*, *reordering*, and *access & layout* (details in Appendix D). Kernel clustering uses scikit-learn’s KMeans with $K = 3$ clusters, a value empirically validated in our experiments; clusters are recomputed every $\tau = 10$ iterations to balance adaptability with computational overhead. For hardware-informed pruning, we use NVIDIA Nsight Compute (NCU) to record throughput metrics (caching results by code hash), and apply a saturation threshold $\theta_{\text{sat}} = 75\%$ to filter strategies that target already-saturated resources. The UCB exploration parameter is $c = 2.0$. These design choices introduce minimal overhead: feature extraction adds less than 1% runtime cost, and clustering incurs negligible cost, scaling as $O(|\mathcal{P}_t|)$ every τ iterations. The dominant costs remain LLM generation and kernel compilation (Section 4.4.1); parameter sensitivity is analyzed in Sections 4.3.1 and 4.5.

4. Experiments

4.1. Experimental Settings

Benchmark. We evaluate on a corrected version of TritonBench-G (Li et al., 2025b), a popular benchmark of GPU Triton kernels (details in Appendix F). After excluding `sin_computation` (which admits trivial simplification yielding artificially high speedups), we obtain 183 kernels spanning 13 functional categories (e.g., attention, matrix multiplication, normalization, fused operations) and 5 difficulty levels (L1-L5).

Hardware platforms. We conduct experiments on three NVIDIA GPUs covering consumer-grade (RTX 4090) and datacenter-grade (H20 and A100) hardware. All platforms run CUDA 12.1 with Triton 3.3.0.

LLM backend. We use DeepSeek-V3.2 (DeepSeek AI, 2025) as the primary LLM backend. Detailed model configurations are provided in Appendix C. We evaluate model generalization with additional backends (OpenAI, 2025; Anthropic, 2025; Google, 2025) in Section 4.3.2.

Baselines. We use: (1) **GEAK** (Wang et al., 2025a), an open-source Triton kernel optimization agent using iterative refinement, with minimal adaptation for our hardware and (2) **Best-of-N (BoN)**, which samples $N = T$ independent variants and selects the fastest (isolating iterative effects). Adaptation details are in Appendix F. We also compare against **PyTorch** baselines, eager execution, `torch.compile` with inductor backend, and `torch.compile` with max-autotune, to contextualize optimization gains with standard PyTorch execution (Appendix G).

Optimization budget. We optimize each kernel for $T = 20$

iterations. Main results (Section 4.2) use this default budget; scaling analysis (Section 4.3.1) extends to $T = 40$ iterations to study convergence behavior.

Evaluation methodology. We adopt TritonBench’s hierarchical evaluation structure. Each task optimizes a single reference kernel over T iterations. Candidates undergo **two-stage correctness verification**: *Call Accuracy* checks for runtime errors, while *Execution Accuracy* verifies numerical equivalence via `torch.allclose`. Passing candidates are benchmarked across 10+ input shapes; per-task speedup is calculated as the **ratio of total runtimes** (baseline over optimized) for the best correct candidate, naturally prioritizing computationally dominant shapes. Details are provided in Appendix H.

Metrics. We report three complementary metrics: (1) **Correct (%)**: Percentage of tasks yielding at least one valid kernel (≥ 1). (2) **Fast@1 (%)**: Percentage of tasks where the best kernel achieves speedup $> 1.0\times$ (failed tasks count as 0). (3) **Geometric Mean Speedup**: Reported in two modes. *Standard mode* (tables) averages only correct tasks to isolate optimization quality. *Fallback mode* (figures) assigns failures and regressions a baseline speedup of $1.0\times$, ensuring monotonic scaling curves and reflecting practical deployment where users fall back to the reference kernel.

4.2. Main Results

Consistent performance dominance. As shown in Table 1, KERNELBAND achieves the highest performance across all GPU architectures. On A100, KERNELBAND attains $1.91\times$ geometric mean speedup with 79.8% correctness, outperforming the best performing baseline, GEAK, by 42.5% in speedup and 66.2% in success rate. Consistent advantages can also be observed on RTX 4090 ($1.74\times$ vs. $1.44\times$) and H20 ($1.45\times$ vs. $1.06\times$).

Robust adaptation via hardware-aware optimization. The most effective kernel optimizations are *hardware-dependent*: the optimal schedule/transform set must reflect each platform’s compute-memory balance and architectural constraints (Williams et al., 2009; Chen et al., 2018; Zheng et al., 2020). Interestingly, KERNELBAND does adapt its optimization choices across devices rather than applying a fixed, hardware-agnostic search policy. For example, compared to H20, KERNELBAND allocates more exploration budget to FUSION on RTX 4090 (18.5% vs. 12.8%), while H20 explores TILING more frequently (10.0% vs. 7.6%). Detailed statistics and analysis can be found in Appendix I. Such platform-specific optimization divergence confirms that our hardware-informed pruning (Assumption 1) effectively calibrates exploration to specific bottlenecks without manual tuning. Consequently, while baseline methods struggle with the diversity (GEAK drops from $1.44\times$ on RTX

Table 1. Performance on TritonBench-G, stratified by difficulty level (L1:easiest, L5:hardest). Adjacent levels are merged where sample sizes are small (L1: 3, L5: 5 kernels) to ensure statistically meaningful aggregation. C: Correct (%). F: Fast@1 (%). G: Geometric mean speedup (standard mode: computed over correct tasks only, including regressions). Best results per configuration in **bold**.

Platform	Method	L1-2			L3			L4-5			All		
		C	F	G	C	F	G	C	F	G	C	F	G
RTX 4090	BoN	63.6	9.1	0.86	12.1	6.1	0.89	28.6	14.3	1.09	31.1	10.0	0.96
	GEAK	68.2	36.4	1.62	21.2	18.2	1.45	80.0	40.0	1.34	55.6	31.1	1.44
	KERNELBAND	81.8	50.0	2.14	60.6	30.3	1.82	91.4	51.4	1.47	77.8	43.3	1.74
H20	BoN	65.5	34.5	1.41	36.9	23.1	1.35	7.1	1.4	0.63	29.3	15.9	0.99
	GEAK	68.9	34.5	1.29	60.0	29.2	1.16	31.4	14.3	0.90	49.4	23.8	1.06
	KERNELBAND	93.1	51.7	1.70	86.2	63.1	1.35	67.1	54.3	1.46	79.3	57.3	1.45
A100	BoN	73.9	34.8	1.43	38.7	24.2	1.23	14.8	6.8	0.76	31.2	16.8	0.98
	GEAK	65.2	43.5	1.09	54.8	45.2	1.18	38.6	33.0	1.54	48.0	38.7	1.34
	KERNELBAND	95.7	82.6	2.23	91.9	77.4	2.05	67.1	42.1	1.75	79.8	60.1	1.91

4090 to $1.06\times$ on H20), KERNELBAND still maintains robust performance ($1.45\times$ to $1.91\times$) across all platforms.

Scaling with kernel complexity. The performance gap widens on challenging kernels. For the 23 **Hard (L4-5)** kernels on A100, KERNELBAND achieves 67.1% correctness and $1.75\times$ speedup, significantly outperforming GEAK (38.6% C, 1.54× G). While naive sampling (BoN) fails to generate valid kernels for 85% of tasks, and unstructured search (GEAK) struggles to improve performance, KERNELBAND’s structured exploration efficiently identifies paths that are both *correct* and *efficient* in the vast search space.

Practical optimization yield. The Fast@1 metric measures the probability of finding an *optimized* kernel (speedup $> 1.0\times$). KERNELBAND demonstrates remarkable consistency, achieving Fast@1 rates of 43.3%–60.1% across all platforms. In contrast, BoN fails to accelerate most tasks (10.0%–16.8%), while GEAK shows both lower average performance and higher volatility (23.8%–38.7%). The 39–140% relative improvement of KERNELBAND over GEAK confirms the effectiveness of our structured exploration: **hardware-informed pruning** filters out physically invalid candidates early, and **dynamic clustering** efficiently guides the search toward high-potential regions. The two algorithmic designs ensure KERNELBAND not only generates correct code but delivers actual speedups for a substantially larger fraction of the optimization budget.

4.3. Detailed Analysis

In this section, We conduct a detailed analysis to validate KERNELBAND’s algorithmic properties, generalization capabilities, and practical cost-efficiency. Unless otherwise stated, all experiments use a 50-kernel subset (preserving category and difficulty distribution as detailed in Appendix E) on the H20 platform.

4.3.1. SCALABILITY AND CLUSTERING SENSITIVITY

We analyze the sample efficiency (i.e., scaling to more iterations) and hyperparameter sensitivity by running KERNELBAND with $K \in \{1, 2, 3, 5\}$ against baselines for an extended budget of $T = 40$ iterations, as shown in Figure 2.

Superior scaling behavior. While baselines saturate early—BoN stagnates at $1.05\times$ and GEAK plateaus at $1.13\times$ after 25 iterations—KERNELBAND ($K=3$) demonstrates continuous improvement, reaching $1.71\times$ at $T=39$. At the standard budget ($T=20$), KERNELBAND achieves $1.48\times$ speedup, outperforming GEAK by 37%. This confirms that our hierarchical MAB solution successfully allows provably efficient exploration for the challenging kernel optimization problem.

Optimal clustering granularity. The interplay between cluster count K and iteration budget reveals a clear trade-off. For limited budgets ($T \leq 10$), smaller $K \in \{1, 2\}$ performs best by concentrating exploration. However, as the budget grows ($T \geq 20$), $K = 3$ overtakes simpler configurations (reaching $1.66\times$ vs. $1.58\times$ for $K = 2$ at $T = 30$). The **5% advantage** demonstrates the value of cross-cluster knowledge transfer when sufficient budget is available. Notably, $K = 5$ consistently underperforms ($1.54\times$), suggesting that excessive fragmentation hurts bandit learning. We therefore recommend $K = 3$ for default optimization. Importantly, all tested K configurations consistently outperform both baselines across the full iteration range, indicating that KERNELBAND’s advantage is robust to this hyperparameter.

4.3.2. ROBUSTNESS ACROSS LLM BACKENDS

To ensure our gains are not model-specific, we benchmark KERNELBAND across four SOTA LLMs.

Generalized performance advantage. As shown in Table 2, KERNELBAND consistently outperforms baselines

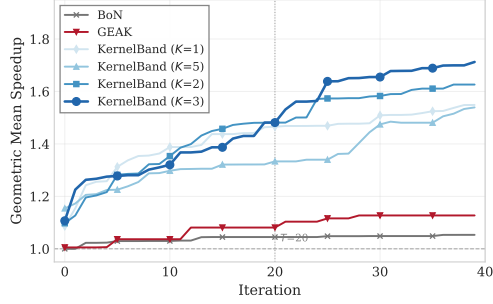


Figure 2. Scaling and clustering sensitivity. KERNELBAND ($K=3$) shows sustained improvement, while baselines saturate early.

Table 2. LLM generalization results. C: Correct (%). G: Geometric mean speedup. F: Fast@1 (%). Best results per model in **bold**.

Model	Method	C (%)	F (%)	G
DeepSeek-V3.2	BoN	27.5	12.5	1.10
	GEAK	37.5	17.5	0.95
	KERNELBAND	85.0	67.5	1.52
GPT-5	BoN	44.9	28.6	1.14
	GEAK	51.0	24.5	1.07
	KERNELBAND	81.6	65.3	1.72
Claude Opus 4.5	BoN	40.8	24.5	1.17
	GEAK	63.3	38.8	1.30
	KERNELBAND	89.8	73.5	1.82
Gemini 3 Flash	BoN	47.9	25.0	1.20
	GEAK	62.5	37.5	1.21
	KERNELBAND	70.8	45.8	1.48

regardless of the underlying model. With Claude Opus 4.5, it achieves an impressive $1.82\times$ speedup and 89.8% correctness. Even with the smaller Gemini 3 Flash, KERNELBAND maintains a substantial lead ($1.48\times$ vs. $1.21\times$ for GEAK).

Compensating for Model Capabilities. While absolute performance naturally correlates with model strength (Claude > GPT-5 > DeepSeek > Gemini), the *relative* gain provided by KERNELBAND remains robust, indicating that our structured exploration framework acts as a powerful amplifier of any code LLM.

4.4. Analysis on the strategy selection pattern.

Strategy risk-reward profiles. Table 3 reveals how the bandit policy manages trade-offs between risks and rewards. **Tiling** represents a “high-risk, high-reward” strategy: low success rate (14.4%) but massive impact when successful (61.5% best-kernel contribution). Conversely, **Vectorization** offers “low-risk, low-reward” gains (57.1% success, 17.1% best). **Fusion** strikes a balance (75% success, 55% best). The bandit policy of KERNELBAND effectively navigates these profiles, prioritizing reliable gains while occasionally gambling on high-variance strategies.

Table 3. Strategy selection statistics. Freq: selection frequency (%). Succ: success rate (%), correct & speedup $>1\times$. Best: percentage of successful applications that contributed to the final best kernel.

Strategy	Freq (%)	Succ (%)	Best (%)
Tiling	10.0	14.4	61.5
Vectorization	14.7	57.1	17.1
Fusion	12.8	75.0	55.2
Pipeline	9.8	64.4	26.3
Reordering	33.2	48.7	25.3
Access & Layout	19.5	29.5	19.2

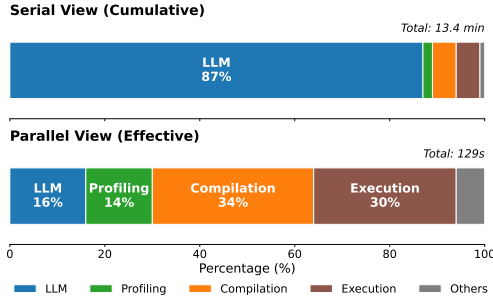


Figure 3. Time breakdown per kernel/iteration: (a) Serial cumulative time (13.4 min); (b) Parallel wall-clock time with batched LLM calls (129s).

4.4.1. COST AND EFFICIENCY ANALYSIS

Finally, we examine the computational and economic feasibility of KERNELBAND for real-world use.

Time breakdown. Figure 3 decomposes the per-kernel iteration latency. While LLM inference dominates serial execution (87%), batched inference shifts the bottleneck to compilation (34%) and execution (30%), reducing the effective wall-clock time to just 129s per iteration. This confirms that KERNELBAND fits comfortably within practical compilation timeouts.

Cost analysis. Despite higher per-iteration costs due to multi-strategy exploration, KERNELBAND delivers superior optimization per dollar as shown in Figure 4. At a fixed budget of \$0.50 per kernel, it achieves $1.83\times$ speedup, outperforming GEAK by 35% ($1.35\times$) and BoN by 50% ($1.22\times$). This cost-effectiveness stems from our pruning mechanism, filtering low-value candidates early, ensuring that API costs translate directly to performance gains.

4.5. Ablation Study

We dissect the effectiveness of KERNELBAND through single-component ablations (removing one module) and framework-level changes (altering the optimization paradigm). Detailed descriptions and analysis of ablation settings can be found in Appendix J.

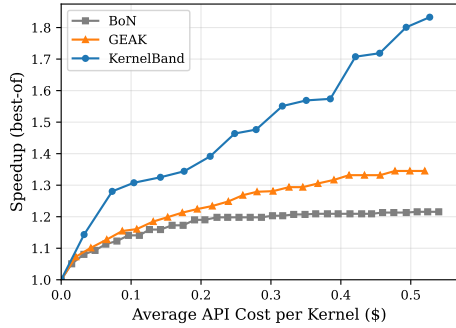


Figure 4. Speedup vs. API cost per kernel. KERNELBAND yields 35-50% higher speedup at equivalent budgets.

Table 4. Single-component ablations show minimal drops; framework-level ablations show the value of core designs.

Type	Configuration	C (%)	F (%)	G
Single	KernelBand (Full)	87.8	63.4	1.57
	w/o Clustering ($K=1$)	82.9	58.5	1.41
	w/o Profiling	85.4	56.1	1.26
	LLM Strategy Selection	68.3	36.6	0.97
Frame.	w/o Strategy + Raw Prof.	43.9	26.8	1.12
	w/o Strategy Set	78.0	48.8	1.15
	BoN (baseline)	34.2	17.1	0.60

Structured bandit policy is foundational. As shown in Table 4, the most critical finding is that replacing bandit-based selection with LLM semantic reasoning (*LLM Strategy Selection*, where a LLM selects which strategy to apply based on kernel analysis rather than using a bandit policy) causes a catastrophic drop to $0.97\times$ speedup. This confirms that learned bandit policy are superior to LLM intuition for strategy selection. Furthermore, removing the strategy set entirely (*w/o Strategy*, where free-form iterative generation is used as GEAK without structured strategies or profiling guidance) drops performance to $1.15\times$. Injecting raw profiling metrics without strategies (*+ Raw Profiling*) introduces noise, further degrading correctness to 43.9%. These results validate that our structured bandit policy is the essential bridge between hardware information and code generation.

Component contribution hierarchy. As shown in Table 4, at the standard budget ($T = 20$), profiling guidance proves more critical than clustering: disabling profiling (*w/o Profiling*) causes a 20% speedup drop ($1.57\times \rightarrow 1.26\times$), while disabling clustering (*w/o Clustering*) yields a 10% drop ($1.41\times$). However, as shown in Section 4.3.1, clustering’s value grows with iteration budget. Both components contribute incrementally to the $2.6\times$ improvement over the BoN baseline ($0.60\times$).

5. Related Work

LLM-based kernel optimization. Several recent and concurrent works explore LLM-based agentic workflows for automated kernel optimization. STARK (Dong et al., 2025a) employs multi-agent collaboration with grounded instruction and strategic search to explore the optimization space. CudaForge (Zhang et al., 2025) uses a Coder-Judge architecture that iteratively generates and refines CUDA kernels with Nsight Compute profiling feedback. GEAK (Wang et al., 2025a) adapts Reflexion-style reasoning loops with inference-time compute scaling for Triton kernel generation. TritonForge (Li et al., 2025a) integrates runtime profiling with iterative code transformation to identify bottlenecks and propose targeted modifications. While these methods demonstrate the value of code LLMs, they lack principled exploration-exploitation mechanisms to effectively navigate the vast optimization space of kernels.

An alternative paradigm focuses on fine-tuning LLMs specifically for kernel generation. ConCuR (Kong et al., 2025) develops a pipeline to generate and curate CUDA kernels with reasoning traces for supervised fine-tuning. Kevin (Baronio et al., 2025) applies multi-turn RL to address challenges in long-trajectory kernel optimization. TritonRL (Woo et al., 2025) combines supervised fine-tuning with RL using hierarchical reward assignment to mitigate reward hacking. Our work is orthogonal to and complement this line of work, as KERNELBAND serves as an amplifier of any given code LLMs demonstrated in our experiment.

Multi-armed bandits and their applications. Multi-armed bandits (MABs) (Berry et al., 1997; Slivkins et al., 2019; Kuleshov & Precup, 2014; Vermorel & Mohri, 2005) provide a principled framework for sequential decision-making under uncertainty, with applications ranging from clinical trials to online advertising (Lai & Robbins, 1985). Classical algorithms like UCB (Auer et al., 2002) and Thompson Sampling (Thompson, 1933) offer optimal regret bounds for stationary environments, while recent work has extended these to contextual (Li et al., 2010; Chu et al., 2011), metric (Kleinberg et al., 2008), clustering (Gentile et al., 2014), and hierarchical settings (Bubeck et al., 2011). In systems optimization, bandit algorithms have shown promise for parameter tuning (Snoek et al., 2012; Pacula et al., 2012), compiler (Xu et al., 2017), and resource allocation (Pandey & Venkatesh, 2025). However, applying bandit algorithms to kernel optimization is largely unexplored, despite the natural fit between the exploration-exploitation trade-off and the challenge of navigating vast optimization spaces.

6. Conclusion

We have introduced KERNELBAND, a framework that bridges the gap between code LLMs and kernel optimization

with a hardware-constrained contextual bandit formulation. By combining runtime behavior clustering with profiling-guided pruning, KERNELBAND enables provably efficient navigation of the vast optimization space. Extensive experiments demonstrate consistent improvements over state-of-the-art methods, achieving up to $1.91\times$ speedup with 39–140% higher optimization Fast@1 across diverse hardware platforms and LLM backends. Our work highlights the importance of structured and hardware-aware exploration to unlocking LLMs’ potential for system optimization.

References

Achiam, J., Adler, S., Agarwal, S., Ahmad, L., Akkaya, I., Aleman, F. L., Almeida, D., Altenschmidt, J., Altman, S., Anadkat, S., et al. Gpt-4 technical report. *arXiv preprint arXiv:2303.08774*, 2023.

Ansel, J., Yang, E., He, H., Gimelshein, N., Jain, A., Voznesensky, M., Bao, B., Bell, P., Berard, D., Burovski, E., et al. Pytorch 2: Faster machine learning through dynamic python bytecode transformation and graph compilation. In *Proceedings of the 29th ACM International Conference on Architectural Support for Programming Languages and Operating Systems, Volume 2*, pp. 929–947, 2024.

Anthropic. Claude Opus 4.5 model card. <https://platform.claude.com/docs/en/resources/overview>, 2025. Accessed: 2026-01; official Claude Opus 4.5 model documentation.

Auer, P., Cesa-Bianchi, N., and Fischer, P. Finite-time analysis of the multiarmed bandit problem. In *Machine learning*, volume 47, pp. 235–256, 2002.

Bai, J., Bai, S., Chu, Y., Cui, Z., Dang, K., Deng, X., Fan, Y., Ge, W., Han, Y., Huang, F., et al. Qwen technical report. *arXiv preprint arXiv:2309.16609*, 2023.

Baronio, C., Marsella, P., Pan, B., Guo, S., and Alberti, S. Kevin: Multi-turn rl for generating cuda kernels. *arXiv preprint arXiv:2507.11948*, 2025.

Berry, D. A., Chen, R. W., Zame, A., Heath, D. C., and Shepp, L. A. Bandit problems with infinitely many arms. *The Annals of Statistics*, 25(5):2103–2116, 1997.

Bouneffouf, D., Rish, I., and Aggarwal, C. Survey on applications of multi-armed and contextual bandits. In *2020 IEEE congress on evolutionary computation (CEC)*, pp. 1–8. IEEE, 2020.

Boursier, E. and Perchet, V. A survey on multi-player bandits. *Journal of Machine Learning Research*, 25(137):1–45, 2024.

Bubeck, S., Munos, R., Stoltz, G., and Szepesvári, C. X-armed bandits. In *Journal of Machine Learning Research*, volume 12, pp. 1655–1695, 2011.

Caruccio, L., Cirillo, S., Polese, G., Solimando, G., Sundaramurthy, S., and Tortora, G. Claude 2.0 large language model: Tackling a real-world classification problem with a new iterative prompt engineering approach. *Intelligent Systems with Applications*, 21:200336, 2024.

Chen, T., Zheng, L., Yan, E., Jiang, Z., Moreau, T., Ceze, L., Guestrin, C., and Krishnamurthy, A. Learning to optimize tensor programs. *Advances in Neural Information Processing Systems*, 31, 2018.

Chu, W., Li, L., Reyzin, L., and Schapire, R. Contextual bandits with linear payoff functions. In *Proceedings of the fourteenth international conference on artificial intelligence and statistics*, pp. 208–214. JMLR Workshop and Conference Proceedings, 2011.

DeepSeek AI. DeepSeek-V3.2 model announcement. <https://api-docs.deepseek.com/news/news251201>, 2025. Accessed: 2026-01; describes DeepSeek-V3.2 model and capabilities.

Dong, J., Feng, B., Guessous, D., Liang, Y., and He, H. Flex attention: A programming model for generating optimized attention kernels. *arXiv preprint arXiv:2412.05496*, 2024.

Dong, J., Yang, Y., Liu, T., Wang, Y., Qi, F., Tarokh, V., Rangadurai, K., and Yang, S. Stark: Strategic team of agents for refining kernels, 2025a. URL <https://arxiv.org/abs/2510.16996>.

Dong, Y., Jiang, X., Qian, J., Wang, T., Zhang, K., Jin, Z., and Li, G. A survey on code generation with llm-based agents. *arXiv preprint arXiv:2508.00083*, 2025b.

Faingnaert, T., Besard, T., and De Sutter, B. Flexible performant gemm kernels on gpus. *IEEE Transactions on Parallel and Distributed Systems*, 33(9):2230–2248, 2021.

Fang, J., Yu, Y., Zhao, C., and Zhou, J. Turbotransformers: an efficient gpu serving system for transformer models. In *Proceedings of the 26th ACM SIGPLAN Symposium on Principles and Practice of Parallel Programming*, pp. 389–402, 2021.

Filipović, J., Madzin, M., Fousek, J., and Matyska, L. Optimizing cuda code by kernel fusion: application on blas. *The Journal of Supercomputing*, 71(10):3934–3957, 2015.

Floridi, L. and Chiriaci, M. Gpt-3: Its nature, scope, limits, and consequences. *Minds and machines*, 30(4):681–694, 2020.

Gao, W., Wang, J., Li, Y., Gao, Y., and Han, L. Automatic parameter selection optimization based on the triton compiler. In *Second International Conference on Power Electronics and Artificial Intelligence (PEAI 2025)*, volume 13657, pp. 1170–1178. SPIE, 2025.

Gentile, C., Li, S., and Zappella, G. Online clustering of bandits. In *International conference on machine learning*, pp. 757–765. PMLR, 2014.

Google. Gemini 3 Flash model endpoint documentation. <https://docs.cloud.google.com/vertex-ai/generative-ai/docs/learn/locations>, 2025. Accessed: 2026-01; lists Gemini 3 Flash in Google GenAI endpoints.

Guo, D., Zhu, Q., Yang, D., Xie, Z., Dong, K., Zhang, W., Chen, G., Bi, X., Wu, Y., Li, Y., et al. Deepseek-coder: When the large language model meets programming—the rise of code intelligence. *arXiv preprint arXiv:2401.14196*, 2024.

Hager, W. W. Lipschitz continuity for constrained processes. *SIAM Journal on Control and Optimization*, 17(3):321–338, 1979.

Hui, B., Yang, J., Cui, Z., Yang, J., Liu, D., Zhang, L., Liu, T., Zhang, J., Yu, B., Lu, K., et al. Qwen2. 5-coder technical report. *arXiv preprint arXiv:2409.12186*, 2024.

Kleinberg, R., Slivkins, A., and Upfal, E. Multi-armed bandits in metric spaces. In *Proceedings of the fortieth annual ACM symposium on Theory of computing*, pp. 681–690, 2008.

Kong, L., Wei, J., Shen, H., and Wang, H. Concur: Conciseness makes state-of-the-art kernel generation. *arXiv preprint arXiv:2510.07356*, 2025.

Kuleshov, V. and Precup, D. Algorithms for multi-armed bandit problems. *arXiv preprint arXiv:1402.6028*, 2014.

Kwon, W., Li, Z., Zhuang, S., Sheng, Y., Zheng, L., Yu, C. H., Gonzalez, J., Zhang, H., and Stoica, I. Efficient memory management for large language model serving with pagedattention. In *Proceedings of the 29th symposium on operating systems principles*, pp. 611–626, 2023.

Lai, T. L. and Robbins, H. Asymptotically efficient adaptive allocation rules. *Advances in applied mathematics*, 6(1): 4–22, 1985.

Lange, R. T., Sun, Q., Prasad, A., Faldor, M., Tang, Y., and Ha, D. Towards robust agentic cuda kernel benchmarking, verification, and optimization. *arXiv preprint arXiv:2509.14279*, 2025.

Li, H., Man, K., Kanuparthi, P., Chen, H., Sun, W., Talam, S., Zhu, C., Zhu, K., and Qian, Z. Tritonforge: Profiling-guided framework for automated triton kernel optimization, 2025a. URL <https://arxiv.org/abs/2512.09196>.

Li, J., Li, S., Gao, Z., Shi, Q., Li, Y., Wang, Z., Huang, J., Wang, H., Wang, J., Han, X., Liu, Z., and Sun, M. Triton-Bench: Benchmarking large language model capabilities for generating triton operators. In *Findings of the Association for Computational Linguistics: ACL 2025*, pp. 23053–23066, Vienna, Austria, jul 2025b. Association for Computational Linguistics. doi: 10.18653/v1/2025. findings-acl.1183. URL [https://aclanthology.org/2025.findings-acl.1183/](https://aclanthology.org/2025.findings-acl.1183).

Li, L., Chu, W., Langford, J., and Schapire, R. E. A contextual-bandit approach to personalized news article recommendation. In *Proceedings of the 19th international conference on World wide web*, pp. 661–670, 2010.

Lin, B., Zhang, C., Peng, T., Zhao, H., Xiao, W., Sun, M., Liu, A., Zhang, Z., Li, L., Qiu, X., et al. Infinite-llm: Efficient llm service for long context with distattention and distributed kvcache. *arXiv preprint arXiv:2401.02669*, 2024.

Mahajan, A. and Teneketzis, D. Multi-armed bandit problems. In *Foundations and applications of sensor management*, pp. 121–151. Springer, 2008.

Miao, X., Oliaro, G., Zhang, Z., Cheng, X., Jin, H., Chen, T., and Jia, Z. Towards efficient generative large language model serving: A survey from algorithms to systems. *ACM Computing Surveys*, 58(1):1–37, 2025.

Naveed, H., Khan, A. U., Qiu, S., Saqib, M., Anwar, S., Usman, M., Akhtar, N., Barnes, N., and Mian, A. A comprehensive overview of large language models. *ACM Transactions on Intelligent Systems and Technology*, 16(5):1–72, 2025.

NVIDIA. NVIDIA Blackwell architecture technical brief, 2025. URL <https://resources.nvidia.com/en-us-blackwell-architecture>.

NVIDIA Corporation. Nvidia nsight compute. <https://developer.nvidia.com/nsight-compute>, 2024. Accessed: 2026-01.

OpenAI. OpenAI gpt-5 announcement. <https://openai.com/index/introducing-gpt-5/>, 2025. Accessed: 2026-01; official GPT-5 model release details.

pacula, M., Ansel, J., Amarasinghe, S., and O'Reilly, U.-M. Hyperparameter tuning in bandit-based adaptive operator selection. In *European Conference on the Applications of Evolutionary Computation*, pp. 73–82. Springer, 2012.

Pan, X., Li, E., Li, Q., Liang, S., Shan, Y., Zhou, K., Luo, Y., Wang, X., and Zhang, J. Instinfer: In-storage attention offloading for cost-effective long-context llm inference. *arXiv preprint arXiv:2409.04992*, 2024.

Pandey, S. and Venkatesh, T. Multi armed bandit based resource allocation in near memory processing architectures. *Memories-Materials, Devices, Circuits and Systems*, pp. 100132, 2025.

Ryoo, S., Rodrigues, C. I., Baghsorkhi, S. S., Stone, S. S., Kirk, D. B., and Hwu, W.-m. W. Optimization principles and application performance evaluation of a multithreaded gpu using cuda. In *Proceedings of the 13th ACM SIGPLAN Symposium on Principles and practice of parallel programming*, pp. 73–82, 2008.

Scott, S. L. A modern bayesian look at the multi-armed bandit. *Applied Stochastic Models in Business and Industry*, 26(6):639–658, 2010.

Shi, Y., Yang, Z., Xue, J., Ma, L., Xia, Y., Miao, Z., Guo, Y., Yang, F., and Zhou, L. Welder: Scheduling deep learning memory access via tile-graph. In *17th USENIX Symposium on Operating Systems Design and Implementation (OSDI 23)*, pp. 701–718, 2023.

Shinn, N., Cassano, F., Berman, E., Gopinath, A., Narasimhan, K., and Yao, S. Reflexion: Language agents with verbal reinforcement learning, 2023.

Silva, N., Werneck, H., Silva, T., Pereira, A. C., and Rocha, L. Multi-armed bandits in recommendation systems: A survey of the state-of-the-art and future directions. *Expert Systems with Applications*, 197:116669, 2022.

Slivkins, A. et al. Introduction to multi-armed bandits. *Foundations and Trends® in Machine Learning*, 12(1-2):1–286, 2019.

Snoek, J., Larochelle, H., and Adams, R. P. Practical bayesian optimization of machine learning algorithms. In *Advances in neural information processing systems*, 2012.

Team, G., Anil, R., Borgeaud, S., Alayrac, J.-B., Yu, J., Soricut, R., Schalkwyk, J., Dai, A. M., Hauth, A., Millican, K., et al. Gemini: a family of highly capable multimodal models. *arXiv preprint arXiv:2312.11805*, 2023.

Team, K., Bai, Y., Bao, Y., Chen, G., Chen, J., Chen, N., Chen, R., Chen, Y., Chen, Y., Chen, Y., et al. Kimi k2: Open agentic intelligence. *arXiv preprint arXiv:2507.20534*, 2025.

Thompson, W. R. On the likelihood that one unknown probability exceeds another in view of the evidence of two samples. *Biometrika*, 25(3-4):285–294, 1933.

Tillet, P., Kung, H.-T., and Cox, D. Triton: an intermediate language and compiler for tiled neural network computations. *Proceedings of the 3rd ACM SIGPLAN International Workshop on Machine Learning and Programming Languages*, pp. 10–19, 2019.

Tschand, A., Awad, M., Swann, R., Ramakrishnan, K., Ma, J., Lowery, K., Dasika, G., and Reddi, V. J. Swizzleperf: Hardware-aware llms for gpu kernel performance optimization. *arXiv preprint arXiv:2508.20258*, 2025.

Vermorel, J. and Mohri, M. Multi-armed bandit algorithms and empirical evaluation. In *European conference on machine learning*, pp. 437–448. Springer, 2005.

Wang, J., Joshi, V., Majumder, S., Chao, X., Ding, B., Liu, Z., Brahma, P. P., Li, D., Liu, Z., and Barsoum, E. Geak: Introducing triton kernel ai agent & evaluation benchmarks. *arXiv preprint arXiv:2507.23194*, 2025a.

Wang, L., Ma, L., Cao, S., Zhang, Q., Xue, J., Shi, Y., Zheng, N., Miao, Z., Yang, F., Cao, T., et al. Ladder: Enabling efficient low-precision deep learning computing through hardware-aware tensor transformation. In *18th USENIX Symposium on Operating Systems Design and Implementation (OSDI 24)*, pp. 307–323, 2024.

Wang, L., Cheng, Y., Shi, Y., Tang, Z., Mo, Z., Xie, W., Ma, L., Xia, Y., Xue, J., Yang, F., et al. Tilelang: A composable tiled programming model for ai systems. *arXiv preprint arXiv:2504.17577*, 2025b.

Williams, S., Waterman, A., and Patterson, D. Roofline: an insightful visual performance model for multicore architectures. *Commun. ACM*, 52(4):65–76, April 2009. ISSN 0001-0782. doi: 10.1145/1498765.1498785. URL <https://doi.org/10.1145/1498765.1498785>.

Woo, J., Zhu, S., Nie, A., Jia, Z., Wang, Y., and Park, Y. Tritonrl: Training llms to think and code triton without cheating. *arXiv preprint arXiv:2510.17891*, 2025.

Xu, C., Liu, G., Zhao, R., Yang, S., Luo, G., and Zhang, Z. A parallel bandit-based approach for autotuning fpga compilation. In *Proceedings of the 2017 ACM/SIGDA international symposium on field-programmable gate arrays*, pp. 157–166, 2017.

Yan, F., He, Y., Ruwase, O., and Smirni, E. Efficient deep neural network serving: Fast and furious. *IEEE Transactions on Network and Service Management*, 15(1):112–126, 2018.

Ye, Z., Chen, L., Lai, R., Lin, W., Zhang, Y., Wang, S., Chen, T., Kasikci, B., Grover, V., Krishnamurthy, A., et al. Flash-infer: Efficient and customizable attention engine for llm inference serving. *arXiv preprint arXiv:2501.01005*, 2025.

Zhang, Z., Wang, R., Li, S., Luo, Y., Hong, M., and Ding, C. Cudaforge: An agent framework with hardware feedback for cuda kernel optimization, 2025. URL <https://arxiv.org/abs/2511.01884>.

Zhao, W. X., Zhou, K., Li, J., Tang, T., Wang, X., Hou, Y., Min, Y., Zhang, B., Zhang, J., Dong, Z., et al. A survey of large language models. *arXiv preprint arXiv:2303.18223*, 1(2), 2023.

Zheng, L., Jia, C., Sun, M., Wu, Z., Yu, C. H., Haj-Ali, A., Wang, Y., Yang, J., Zhuo, D., Sen, K., et al. Ansor: Generating high-performance tensor programs for deep learning. In *14th USENIX symposium on operating systems design and implementation (OSDI 20)*, pp. 863–879, 2020.

Zhu, H., Wu, R., Diao, Y., Ke, S., Li, H., Zhang, C., Xue, J., Ma, L., Xia, Y., Cui, W., et al. Roller: Fast and efficient tensor compilation for deep learning. In *16th USENIX Symposium on Operating Systems Design and Implementation (OSDI 22)*, pp. 233–248, 2022.

A. Implementation Details

A.1. Profiling and Clustering Features

Behavioral feature vector $\phi(k)$. As defined in Section 3.2, we extract a 5-dimensional vector for clustering kernels with similar optimization responses:

- $\tilde{\mathcal{T}}(k)$: normalized execution time (from timing run, log-transformed)
- n_{reg} : registers per thread (from `cuFuncGetAttribute`)
- n_{smem} : shared memory per block (from `cuFuncGetAttribute`)
- d_{block} : block dimensions (from launch configuration)
- η_{occ} : theoretical occupancy (computed via `cudaOccupancyMaxActiveBlocksPerMultiprocessor`)

Hardware signature $h(k)$. For hardware-aware pruning, we extract throughput metrics via NVIDIA Nsight Compute to identify resource saturation:

- SM throughput (`sm__throughput.avg.pct_of_peak_sustained_elapsed`)
- DRAM throughput (`dram__throughput.avg.pct_of_peak_sustained_elapsed`)
- L2 throughput (`lts__throughput.avg.pct_of_peak_sustained_elapsed`)

These three metrics correspond to the compute, memory bandwidth, and cache bottleneck categories described in Section 3.2.

B. Proof of Theorem 1

In this section, we provide the detailed derivation for the convergence bound of KERNELBAND.

B.1. Regret Decomposition

Let $x^* = \arg \max_{x \in \mathcal{X}} \mu(x)$ be the global optimal kernel configuration with expected reward μ^* . Let x_{disc}^* be the best candidate available in our discretized cluster centers, i.e., $x_{\text{disc}}^* = \arg \max_{c \in \{C_1, \dots, C_K\}} \mu(c)$.

The cumulative regret $R(T)$ after T rounds can be decomposed into *Approximation Regret* (R_{approx}) and *Estimation Regret* (R_{est}):

$$R(T) = \sum_{t=1}^T (\mu^* - \mu(x_t)) \tag{8}$$

$$= \sum_{t=1}^T (\mu^* - \mu(x_{\text{disc}}^*) + \mu(x_{\text{disc}}^*) - \mu(x_t)) \tag{9}$$

$$= \underbrace{T \cdot (\mu^* - \mu(x_{\text{disc}}^*))}_{R_{\text{approx}}} + \underbrace{\sum_{t=1}^T (\mu(x_{\text{disc}}^*) - \mu(x_t))}_{R_{\text{est}}} \tag{10}$$

B.2. Bounding Approximation Regret

Based on Assumption 2 (Lipschitz Continuity), the performance function $\mu(\cdot)$ is L -Lipschitz. Since our clustering algorithm covers the space such that for any x , there exists a cluster center c with $\|x - c\| \leq \epsilon$, the gap between the global optimum and the best discrete representative is bounded by:

$$\mu^* - \mu(x_{\text{disc}}^*) \leq L \cdot \|x^* - x_{\text{disc}}^*\| \leq L\epsilon$$

Therefore:

$$R_{\text{approx}} \leq T \cdot L\epsilon \tag{11}$$

B.3. Bounding Estimation Regret

The term R_{est} represents the regret incurred by a Multi-Armed Bandit (MAB) algorithm selecting among K clusters (and their associated strategies $|\mathcal{S}|$). The total number of arms is $N = K|\mathcal{S}|$. For standard UCB algorithms, the regret is bounded by $\tilde{O}(\sqrt{NT})$. Specifically, with probability $1 - \delta$:

$$R_{est} \leq \sqrt{C \cdot K|\mathcal{S}|T \log(T/\delta)} \quad (12)$$

for some universal constant C .

B.4. Final Average Regret Bound

Combining the bounds for R_{approx} and R_{est} :

$$R(T) \leq O\left(\sqrt{K|\mathcal{S}|T \log T}\right) + L\epsilon T$$

Dividing by T to obtain the average regret (convergence rate):

$$\frac{R(T)}{T} \leq O\left(\sqrt{\frac{K|\mathcal{S}| \log T}{T}}\right) + L\epsilon$$

As $T \rightarrow \infty$, the first term approaches 0, ensuring that the algorithm converges to the $L\epsilon$ -neighborhood of the global optimum.

C. LLM Configuration

Table 5 summarizes the configuration for all LLM backends used in our experiments.

Table 5. LLM backend configurations.

Parameter	Value
Primary Model	DeepSeek-V3.2
Access Method	Official API
Temperature	1.0
Max Output Tokens	16384

D. Optimization Strategy Set

Table 6 provides the complete list of optimization strategies in \mathcal{S} with their descriptions and example transformations.

Table 6. Complete optimization strategy set. This refined set was distilled from an initial 10 strategies through pilot experiments.

Strategy	Description
Tiling	Partition computation into configurable tile sizes for improved cache locality and parallelism
Vectorization	Use vector loads/stores (e.g., float4) for improved memory throughput
Fusion	Combine multiple operations to reduce intermediate memory traffic
Pipeline	Configure software pipelining depth for latency hiding
Reordering	Optimize loop order and instruction scheduling for better ILP
Access & Layout	Optimize memory access patterns, coalescing, and data layout

Table 7. Category distribution: full benchmark vs. sampled subset.

Category	Full (184)	Subset (50)
Attention	29 (15.8%)	7 (14.0%)
MatMul/GEMM	26 (14.1%)	7 (14.0%)
Normalization	18 (9.8%)	4 (8.0%)
Linear Attention/SSM	17 (9.2%)	4 (8.0%)
Element-wise Ops	16 (8.7%)	3 (6.0%)
Memory/Index Ops	13 (7.1%)	3 (6.0%)
Other	12 (6.5%)	3 (6.0%)
Embedding/RoPE	11 (6.0%)	3 (6.0%)
Softmax	11 (6.0%)	4 (8.0%)
Fused Ops/Activation	10 (5.4%)	4 (8.0%)
Quantization	8 (4.3%)	2 (4.0%)
Loss Functions	7 (3.8%)	3 (6.0%)
Reduction	6 (3.3%)	3 (6.0%)

E. Benchmark Subset Details

For detailed analysis experiments, we use a stratified subset of 50 kernels from the 184-kernel TritonBench-G benchmark. The subset was generated using stratified random sampling (seed=42) to preserve the original category and difficulty distribution:

- **Category coverage:** All 13 functional categories represented
- **Difficulty distribution:** L1 (1), L2 (7), L3 (18), L4 (23), L5 (1)
- **Sampling ratio:** 27.2% of the full benchmark
- **Maximum deviation from original distribution:** <1%

Table 7 compares the category distribution between the full benchmark and the sampled subset. Table 8 lists all 50 kernels organized by difficulty level and functional category.

F. Baseline Discussion

Benchmark Modifications. The original TritonBench release contained implementation issues that impacted reliable evaluation. We adopt the corrected benchmark version provided by GEAK (Wang et al., 2025a), which addresses these issues. Additionally, we performed straightforward function substitutions to convert AMD-specific implementations to their NVIDIA equivalents, without modifying kernel logic or semantics.

GEAK Adaptation. GEAK’s adaptation to NVIDIA GPUs involved only platform-specific configurations (e.g., device queries, memory bandwidth specifications) without altering the agent’s core logic or prompts.

Other Agent-based Methods. Other agent-based methods present reproducibility challenges: STARK (Dong et al., 2025a), TritonForge, and QiMeng-Kernel have not released their code; we contacted authors but code remains unavailable due to corporate IP constraints or ongoing submissions. CudaForge (Zhang et al., 2025) targets CUDA kernels on KernelBench and would require non-trivial adaptation to our Triton-based evaluation framework; we consider it concurrent work.

G. PyTorch Baseline Comparison

To contextualize the optimization gains of Triton kernels relative to standard PyTorch execution, we compare KERNELBAND-optimized kernels against three PyTorch execution modes: (1) **eager** mode (default PyTorch execution), (2) **inductor** (`torch.compile` with the default inductor backend), and (3) **max-autotune** (`torch.compile` with `mode="max-autotune"`).

Experimental setup. From the 50-kernel subset, we select 30 kernels suitable for fair comparison with PyTorch, where native operators are available (e.g., `torch.softmax`, `F.layer_norm`). We exclude special-purpose kernels (e.g., Flash

Attention decode, INT4 quantization, LoRA operations) that lack general PyTorch counterparts. Experiments are conducted on H20 with DeepSeek-V3.2 and $T = 20$ iterations.

Results. Table 9 presents the geometric mean speedup of KERNELBAND-optimized Triton kernels over each PyTorch baseline. The results demonstrate that KERNELBAND achieves substantial speedups over all PyTorch execution modes, with $1.87\times$ over inductor, $2.16\times$ over max-autotune, and $2.13\times$ over eager execution. The larger speedup over max-autotune compared to inductor is noteworthy: while max-autotune performs more extensive autotuning, it may over-specialize to specific input shapes, whereas KERNELBAND’s optimization generalizes better across the diverse input shapes in our evaluation.

These results validate that KERNELBAND’s LLM-driven Triton kernel optimization provides meaningful performance gains beyond what PyTorch’s built-in compilation and autotuning can achieve, justifying the investment in custom kernel development for performance-critical workloads.

H. Evaluation Protocol Details

Correctness verification. The *Execution Accuracy* check uses `torch.allclose` with absolute tolerance $\text{atol} = 10^{-4}$ and relative tolerance $\text{rtol} = 10^{-4}$. A kernel passes when $|\text{generated} - \text{reference}| \leq \text{atol} + \text{rtol} \times |\text{reference}|$.

Statistical robustness. For each input shape, we use Triton’s `triton.testing.do_bench` function, which handles common GPU benchmarking pitfalls such as measuring only kernel launch time (via `time.time`), omitting cache clearing, and skipping warmup. The function performs 100ms of warmup runs to stabilize GPU state, followed by 1000ms of timed runs. We report the median execution time to reduce sensitivity to outliers.

Weighted aggregation. The overall kernel speedup is computed as the ratio of total baseline runtime to total optimized runtime:

$$\text{Speedup} = \frac{\sum_i t_{\text{baseline},i}}{\sum_i t_{\text{optimized},i}}$$

This metric reflects end-to-end performance: shapes with longer execution times naturally dominate the aggregation.

I. Robust adaptation to hardware diversity

Prior work has repeatedly shown that the most effective operator optimizations are *hardware dependent*: the optimal schedule/transform set must reflect each platform’s compute–memory balance and microarchitectural constraints (e.g., cache behavior, memory bandwidth, and parallel execution resources) (Williams et al., 2009; Chen et al., 2018; Zheng et al., 2020). Consistent with this principle, our empirical strategy statistics provide direct evidence that KERNELBAND adapts its optimization choices across devices rather than applying a fixed, hardware-agnostic search policy. Table 10 reports three complementary views: (i) selection frequency (FREQ), (ii) success rate among attempted transformations (SUCC; correctness and speedup $> 1\times$), and (iii) contribution to the final best kernel (BEST). The observed shifts in FREQ across H20 and RTX 4090 indicate that KERNELBAND reallocates exploration budget across strategy families in a platform-aware manner, aligning with the long-standing motivation behind hardware-targeted auto-scheduling systems (Chen et al., 2018; Zheng et al., 2020).

Concretely, the strategy mix differs noticeably between H20 and RTX 4090. For example, FUSION is selected substantially more often on RTX 4090 (FREQ 18.5%) than on H20 (12.8%), and it remains highly reliable on both devices (SUCC 78.6% on RTX 4090 vs. 75.0% on H20), while also contributing frequently to the best-performing kernels (BEST 63.1% vs. 55.2%). In contrast, TILING exhibits an inverse risk–reward profile: it is attempted slightly more on H20 (10%) than on RTX 4090 (7.6%), yet has low success rates on both (14.4% vs. 18.7%) while yielding disproportionately large best-kernel contributions when it does succeed (BEST 61.5% on H20 vs. 47.3% on RTX 4090). Meanwhile, ACCESS & LAYOUT becomes more prominent on RTX 4090 (22.9% vs. 19.5%) and shows higher effectiveness there (SUCC 38.9% vs. 29.5%), suggesting device-specific sensitivity to memory access behavior and layout-driven locality. These cross-device changes collectively support our claim that KERNELBAND calibrates its search to the dominant bottlenecks of each platform, as predicted by performance modeling insights (e.g., Roofline) and confirmed by hardware-aware optimization studies (Williams et al., 2009; Tschand et al., 2025).

J. Detailed Ablation Study

J.0.1. COMPONENT ABLATION

To understand the contribution of each component, we evaluate KERNELBAND with seven configurations organized into two categories: *single-component ablations* that remove one component while preserving others, and *framework-level ablations* that alter the fundamental optimization paradigm.

Single-component ablations. These configurations isolate the contribution of individual components:

- **KernelBand (Full):** Complete system with strategy set, hardware-aware masking and kernel selection, UCB-based exploration, and runtime clustering ($K = 3$).
- **w/o Clustering** ($K = 1$): All kernels treated as a single cluster. Tests whether runtime-behavior clustering enables effective cross-kernel knowledge transfer.
- **w/o Profiling:** Hardware masking disabled ($M_{i,s} = 1$ for all), and within-cluster kernel selection falls back to recency tie-break. Tests the value of hardware profiling guidance.
- **LLM Strategy Selection:** Strategy set preserved, but the LLM selects which strategy to apply based on kernel analysis rather than UCB statistics. Tests whether learned statistics outperform LLM semantic judgment.

Framework-level ablations. These configurations fundamentally alter how optimization is structured:

- **w/o Strategy + Raw Profiling:** Removes the strategy set; the LLM generates optimizations freely with raw profiling metrics (L2 miss rate, memory bandwidth, etc.) injected into the prompt. Tests structured strategy abstraction versus raw metric injection (Zhang et al., 2025).
- **w/o Strategy Set:** Free-form iterative generation without structured strategies or profiling guidance, similar to Reflexion-style approaches (Shinn et al., 2023). Since the strategy set is foundational to UCB statistics and profiling compatibility, removing it effectively disables these components.
- **BoN (baseline):** Best-of-N independent sampling without iteration. Included as a lower bound to quantify the value of iterative optimization.

Component dependencies. An important insight is that the strategy set \mathcal{S} serves as the foundation for other components: profiling computes compatibility $\psi(s, \phi(k))$ per strategy, UCB maintains statistics $\hat{\mu}_{i,s}$ per (cluster, strategy) pair, and clustering's primary value is enabling cross-cluster UCB statistic sharing. Thus, removing the strategy set (framework-level ablation) implicitly disables structured use of profiling and UCB, which is why we expect a larger performance gap for framework-level ablations compared to single-component ablations.

Table 8. Complete list of 50 kernels in the evaluation subset, stratified by difficulty (L1–L5) and functional category.

#	Diff.	Category	Kernel Name
1	L1	Element-wise Ops	cosine_compute
2	L2	Attention	flash_decode2_phi
3	L2	MatMul/GEMM	matmul_kernel
4	L2	Memory/Index Ops	matrix_transpose
5	L2	Normalization	triton_mul2
6	L2	Other	square_matrix
7	L2	Reduction	triton_argmax
8	L2	Softmax	softmax_triton1
9	L3	Attention	flash_decode2_llama
10	L3	Element-wise Ops	pow_scalar_tensor
11	L3	Embedding/RoPE	embedding_triton_kernel
12	L3	Fused Ops/Activation	relu_strided_buffer
13	L3	Fused Ops/Activation	swiglu_backward
14	L3	Fused Ops/Activation	swiglu_triton
15	L3	Linear Attention/SSM	chunk_cumsum_vector
16	L3	Linear Attention/SSM	reversed_cumsum_scalar
17	L3	Loss Functions	kldiv_triton
18	L3	MatMul/GEMM	triton_matmul
19	L3	Memory/Index Ops	var_len_copy
20	L3	Normalization	layer_norm_welfold
21	L3	Normalization	rmsnorm_fused_llama
22	L3	Other	uniform_sampling
23	L3	Quantization	quantize_kv_copy
24	L3	Reduction	matrix_reduction
25	L3	Softmax	softmax_triton2
26	L3	Softmax	softmax_triton3
27	L4	Attention	attention_fwd_triton1
28	L4	Attention	attention_fwd_triton2
29	L4	Attention	attention_kernel
30	L4	Attention	triton_attention
31	L4	Element-wise Ops	matrix_vector_multip
32	L4	Embedding/RoPE	fast_rope_embedding
33	L4	Embedding/RoPE	rope_backward_transform
34	L4	Fused Ops/Activation	relu_triton_kernel
35	L4	Linear Attention/SSM	chunk_gate_recurrence
36	L4	Linear Attention/SSM	fused_recurrent_retention
37	L4	Loss Functions	cross_entropy_ops
38	L4	Loss Functions	fast_ce_loss
39	L4	MatMul/GEMM	int8_matmul_quantization
40	L4	MatMul/GEMM	int_scaled_matmul
41	L4	MatMul/GEMM	matmul_dequantize_int4
42	L4	MatMul/GEMM	rms_matmul_rbe
43	L4	MatMul/GEMM	streamk_matmul
44	L4	Memory/Index Ops	kcache_copy_triton
45	L4	Normalization	fused_layernorm_triton
46	L4	Other	bgmv_expand_slice
47	L4	Quantization	quantize_copy_kv
48	L4	Reduction	logsumexp_fwd
49	L4	Softmax	ksoftmax_triton
50	L5	Attention	context_attn_bloom

Table 9. Speedup of KERNELBAND-optimized Triton kernels over PyTorch baselines (30 kernels, H20, $T = 20$).

PyTorch Baseline	Speedup
vs. eager	2.13 \times
vs. inductor	1.87 \times
vs. max-autotune	2.16 \times

Table 10. Strategy utilization statistics across H20 and RTX 4090 (50 kernels, $T=20$). FREQ: selection frequency (%). SUCC: success rate (%), correct and speedup $> 1\times$. BEST: percentage of successful applications that contributed to the final best kernel.

(a) H20				(b) RTX 4090			
Strategy	Freq (%)	Succ (%)	Best (%)	Strategy	Freq (%)	Succ (%)	Best (%)
Tiling	10	14.4	61.5	Tiling	7.6	18.7	47.3
Vectorization	14.7	57.1	17.1	Vectorization	16.2	61.4	14.6
Fusion	12.8	75.0	55.2	Fusion	18.5	78.6	63.1
Pipeline	9.8	64.4	26.3	Pipeline	5.7	51.9	13.8
Reordering	33.2	48.7	25.3	Reordering	29.1	49.8	30.7
Access & Layout	19.5	29.5	19.2	Access & Layout	22.9	38.9	35.9